



## Comparison between mass spectra of individual organic particles generated by UV laser ablation and in the IR/UV two-step mode

Alla Zelenyuk<sup>a,\*</sup>, Juan Yang<sup>a</sup>, Dan Imre<sup>b</sup>

<sup>a</sup> Pacific Northwest National Laboratory, Richland, WA 99354, United States

<sup>b</sup> Imre Consulting, Richland, WA 99352, United States

### ARTICLE INFO

#### Article history:

Received 25 September 2008

Received in revised form 24 January 2009

Accepted 26 January 2009

Available online 6 February 2009

#### Keywords:

Single particle mass spectrometry

Laser desorption

Laser ionization

### ABSTRACT

In ablation-based single particle mass spectrometry it is common to find that the mass spectra of particles with identical compositions exhibit significant particle-to-particle fluctuations and high degree of fragmentation. This is particularly true when it comes to particles containing organic compounds. At laser fluence that is sufficient to ionize sulfates, mass spectra of the identical organic particles are classified into multitude of classes, some of which are indistinguishable from elemental carbon. In contrast, the individual particle mass spectra generated in two-step mode, in which an IR laser pulse is used to evaporate the semivolatile particle components and a time delayed UV laser pulse is used to ionize the evaporating plume, exhibit greatly diminished particle-to-particle fluctuations and significantly improved mass spectral quality. Since individual particle mass spectra must first be classified and only then can be averaged and analyzed, the IR/UV mode greatly improves the capability to properly quantify particle compositions. We present an experimental investigation of the properties and behavior of individual particle mass spectra of organic particles that are generated by ablation and in the two-step mode as function of UV laser fluence and the delay between the two lasers. The study shows that the two-step mode yields highly reproducible mass spectra that contain sufficient detail to allow molecular identification. In addition it produces significantly higher mass spectral intensities that are linearly related to the mass of organics in the particles. In contrast, ablation generated mass spectra were found to exhibit high degree of fragmentation and large particle-to-particle fluctuations.

© 2009 Elsevier B.V. All rights reserved.

### 1. Introduction

Single Particle Mass Spectrometers (SPMSs) have been developed to characterize, in real-time, the size and internal composition of *individual* ambient particles [1–8]. One of the criticisms of these instruments has been their inability to properly identify the composition of the organic fraction in atmospheric aerosols and even to distinguish between elemental and organic carbon. This issue has recently come to the forefront because field measurements indicate that organic aerosols represent a significant fraction of the atmospheric aerosol composition, accounting for 20–90% of the total atmospheric dry aerosol mass [9,10].

A number of recent reviews and tutorials provide detailed descriptions and comparisons between the available SPMSs [1–8]. Aside from SPLAT II instrument [11] all field deployable SPMSs use pulsed ultraviolet (UV) lasers to ablate the particles to produce ions

that are subsequently analyzed with time-of-flight mass spectrometers (TOF-MS) [12–19]. Examinations of the ablation generated individual particles mass spectra reveal significant challenges that need to be overcome: the mass spectra generated by ablation, a highly non-linear, multi-photon process, are strongly influenced by matrix and charge transfer effects [20–24], exhibit extensive fragmentation of organic molecules, and significant particle-to-particle fluctuations of mass spectral peak intensities.

One of the most fundamental aspects of single particle mass spectrometry is that the individual particle mass spectra have to be first classified and only then can be averaged and analyzed. But, because ablation generated mass spectra exhibit significant particle-to-particle variability, the mass spectra of identical particles are often separated during the classification process [25,26]. Similarly, extensive fragmentation of organic particles makes them indistinguishable from elemental carbon and consequently a significant fraction of the particles that are composed of organic compounds end up being erroneously classified as soot.

In ablation the degree of fragmentation is strongly dependent on the laser fluence. Reducing laser fluence may decrease degree of fragmentation for organic compounds, but inevitably leads to the instrument's inability to detect important atmospheric

\* Corresponding author at: Pacific Northwest National Laboratory, Chemical Structure & Dynamics, 3335 Q Avenue, K8-88, Richland, WA 99354, United States. Tel.: +1 509 3716155.

E-mail address: [alla.zelenyuk@pnl.gov](mailto:alla.zelenyuk@pnl.gov) (A. Zelenyuk).

constituents such as sulfuric acid, ammonium sulfate, and others [27,28]. The laser wavelength also plays an important role—longer wavelengths require more photons and inevitably yield more fluctuations and higher degree of fragmentation [29].

Separation between particle evaporation and ion formation was shown to greatly improve the analytical capability of SPMS [30–35]. Morrical et al. [32] have shown that the mass spectra of semivolatile particle constituents, which were first evaporated with an IR laser pulse and subsequently ionized in the gas phase, exhibit significantly decreased degree of fragmentation. Lazar et al. [36] used two, time delayed, UV laser pulses to analyze particles' surface compositions. The first excimer laser pulse at 308 nm was used to desorb the semivolatile components and the second pulse at 248 nm was used to ionize the evaporating compounds. The authors concluded that this approach yields higher ion signals and reduced fragmentation.

Zelenyuk et al. [37] and Cabalo et al. [31] investigated the behavior of the mass spectral signal intensity as a function of delay between a CO<sub>2</sub> laser, used to evaporate ~2.4 μm particles composed of aniline, and an excimer laser at 193 nm, used to ionize the evaporating plume. They found that the ion intensities of mass spectra generated in the IR/UV mode with delays between 2.5 μs and 4 μs are more than two orders of magnitude higher than the ion intensities of mass spectra produced by ablation. A series of subsequent articles by the same research group [35,38,39] describe the use of a number of IR and UV sources and conclude that mass spectra of organic particles generated by the two-step process exhibit a lower degree of fragmentation. It is important to note that in each of these reports the authors presented only mass spectra that were averaged over many particles.

In an earlier publication [33] we provided an illustrative example, in which we compared mass spectra of individual particles composed of succinic acid that were generated by UV laser ablation and those generated in the IR/UV mode, to qualitatively demonstrate that unlike ablation, the two-step mode produces size-independent individual particle mass spectra.

Our goal here is to compare the properties of the *individual* mass spectra of organic particles that are generated by ablation and by the IR/UV mode at different UV laser fluences, particularly those required to characterize all ambient atmospheric particles. We perform the experiments on size-selected particles composed of dioctyl phthalate (DOP) with precisely controlled diameters between 250 nm and 500 nm. Data are analyzed using SpectraMiner—our data classification, analysis and visualization software [25] with parameters identical to those used to analyze field data.

## 2. Experimental

DOP particles were generated by aerosolizing neat DOP (Aldrich, 99% purity) using an atomizer (TSI Inc., Model 3076). The particles were classified with a Differential Mobility Analyzer (DMA, TSI Inc., Model 3081) at 163 nm yielding multiply charged particles with diameters of 256 nm, 341 nm, 421 nm and 500 nm and sampled by our single particle mass spectrometer, SPLAT II [11].

SPLAT II is described in detail elsewhere [11]. Here we note only some of the relevant aspects. SPLAT II uses an aerodynamic lens inlet to efficiently transport particles into the vacuum system, where particle vacuum aerodynamic diameters are determined on the basis of the particle's time of flight between two optical detection stages that are 10.5 cm apart. The IR, CO<sub>2</sub> laser (Edinburgh Instruments, Model MTL-3, 50 ns pulse length, 10.6 μm wavelength) and UV, excimer laser (GAM Lasers, Model EX5/300, 8 ns pulse length, 193 nm wavelength) beams intersect the particle beam 10.5 cm downstream from the second optical detection stage, at the ion source region of the angular reflectron time-of-flight mass spectrometer (TOF-MS, R.M. Jordan, Inc., Model D-850). The IR laser

beam is focused down to a 1 mm spot and the UV laser is focused to a spot that is 550 μm by 750 μm that is positioned 50 μm downstream of the IR laser beam. This distance translates, for 300 nm DOP particles, to a flight time of 0.5 μs between the two laser beams. The IR laser pulse is timed to coincide with the particle's arrival into the center of its focal spot and the UV laser pulse is delayed to allow the evaporating plume to expand. The time delay between the two lasers is varied and its effect on the mass spectra is explored and discussed below.

We find that in this configuration a delay of ~5 μs yields excellent results for all UV laser fluences and all particle sizes used in the study. At this delay the UV laser pulse misses the particle center of mass and ionizes the “back-edge” of the evaporating plume. There is clearly a range of possible arrangements, in which the two lasers can be positioned, giving the operator the option to tailor the system for specific applications. The present study is intended to explore the characteristics of the individual particle mass spectra that are generated in the IR/UV mode by UV ionization of the gas phase only.

The acquired individual particle mass spectra are analyzed using SpectraMiner [25], a software package that was designed for classification, visualization and analysis of large datasets generated by single particle mass spectrometers. The details of SpectraMiner are presented in separate publication [25], here we outline only the relevant aspects.

The first step involves data reduction, in which the recorded ions' time-of-flights are converted into the corresponding integer mass-to-charge ( $m/z$ ) ratios and the areas under each of the peaks are calculated by integrating the intensities within ±0.5 Da of each of the 450  $m/z$  values. The mass spectra are then examined and separated into hits and misses, representing particle and background gas mass spectra, respectively. In the present experiment the hit-rates, which are defined as the ratio of the number of particle hits to the number of optically detected and sized particles, vary between 50% and 100%, depending on the delay time between the two lasers and on the UV laser fluence.

One of the most important aspects of the present study is to subject these laboratory-generated individual particle mass spectra to the very same process that is used for field data. Thus the reduced data are classified here using SpectraMiner with a distance threshold identical to that used to classify field data. This threshold was originally chosen to assure the ability to distinguish between the mass spectra of particles composed of ammonium sulfate and ammonium nitrate, and particles containing different internal mixtures of sulfates and organics that are often found in atmospheric particles [40]. The classified data are visualized in a form of an interactive circular hierarchical tree. In the present case ~12,000 individual particle mass spectra generated under different conditions that include a range of UV laser fluences, time delays, and particle sizes are classified together to yield 12 distinct classes.

In a recent study that focuses on the classification of ablation generated single particle mass spectra [25] we showed that the mass spectra of organic compounds tend to exhibit a wide range of fragmentation patterns, and as result particles with identical compositions are being classified into a large number of classes. The goal here is to develop better understanding of the relationship between the experimental conditions, under which the data are generated, and the number and types of classes the data are classified into.

## 3. Results and discussion

### 3.1. Low UV laser fluence

We start with an examination of individual particle mass spectra that are generated with UV laser fluence of 0.09 J/cm<sup>2</sup>, which is just slightly above the threshold for DOP particle laser ablation.

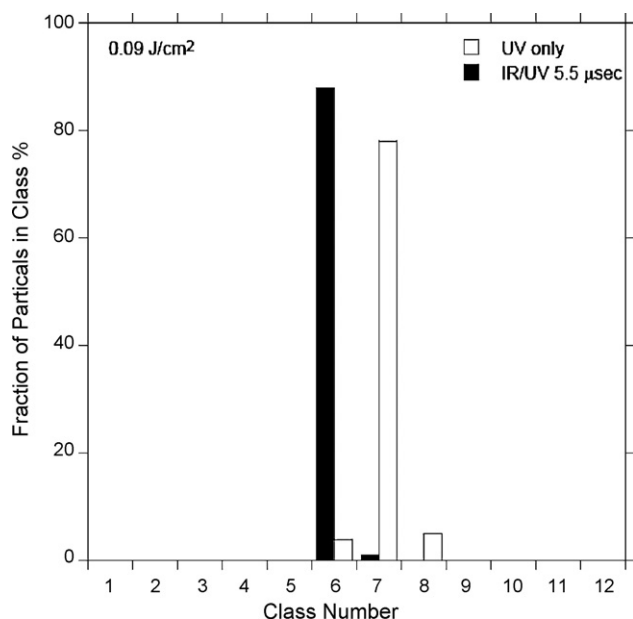


**Fig. 1.** The classification results of mass spectra generated by ablation and in the IR/UV mode at a UV laser fluence of  $0.09 \text{ J/cm}^2$ .

**Fig. 1** displays the classification results of the data generated at this low UV laser fluence by ablation and in the IR/UV mode with a time delay of  $5.5 \mu\text{s}$ . The figure shows that in this case 78% of ablation generated mass spectra are classified into class 7 and the rest belong to nearby classes and, by comparison, over 90% of mass spectra generated the IR/UV mode belong to class 6. The average mass spectra of particles classified in classes 6 and 7 are shown in **Fig. 2** along with the reference, 70 eV electron impact ionization mass spectrum of DOP from the NIST Standard Reference Database. A comparison between these three mass spectra shows remarkable similarity, with the most intense peak being at characteristic for the phthalates  $m/z$  ratio of 149 ( $\text{C}_6\text{H}_4(\text{CO})_2\text{OH}^+$ ). Moreover, the fact that the majority of the individual particle mass spectra are classified into a single cluster in either of the ion generation methods suggests that at least for DOP, at low laser power, UV laser ablation could be used to generate high quality single particle mass spectra.

However, our previous experience with NaCl particles coated with DOP showed that this laser fluence is insufficient to penetrate a DOP layer that is 36 nm thick and is therefore useful only for characterizing the particle's surface composition [20]. It is also a factor of 6 lower than the power needed to ionize substances like ammonium sulfate.

In **Fig. 3** we present the measured averaged integrated peak intensities per particle for mass spectra generated by ablation and in the IR/UV mode as a function of delay time between the IR and UV lasers. Here, the data are separated into the 4 particle sizes. An examination of the mass spectra generated in the IR/UV mode with a time delay of  $0.5 \mu\text{s}$  shows that this short time is insufficient to allow the particles to evaporate and the mass spectra appear to be nearly identical to those generated by laser ablation. **Fig. 3** shows that the mass spectral intensity increases with delay time peaking, for this laser power, at a delay of  $\sim 3.5 \mu\text{s}$  and then decreases as the delay increases.

### 3.2. Medium UV laser fluence

When the laser power is increased by approximately a factor of three, to  $0.31 \text{ J/cm}^2$ , the laser ablation generated mass spectra change significantly, yet this laser fluence is still too low to be useful for most field deployments. In **Fig. 4** we present the results of

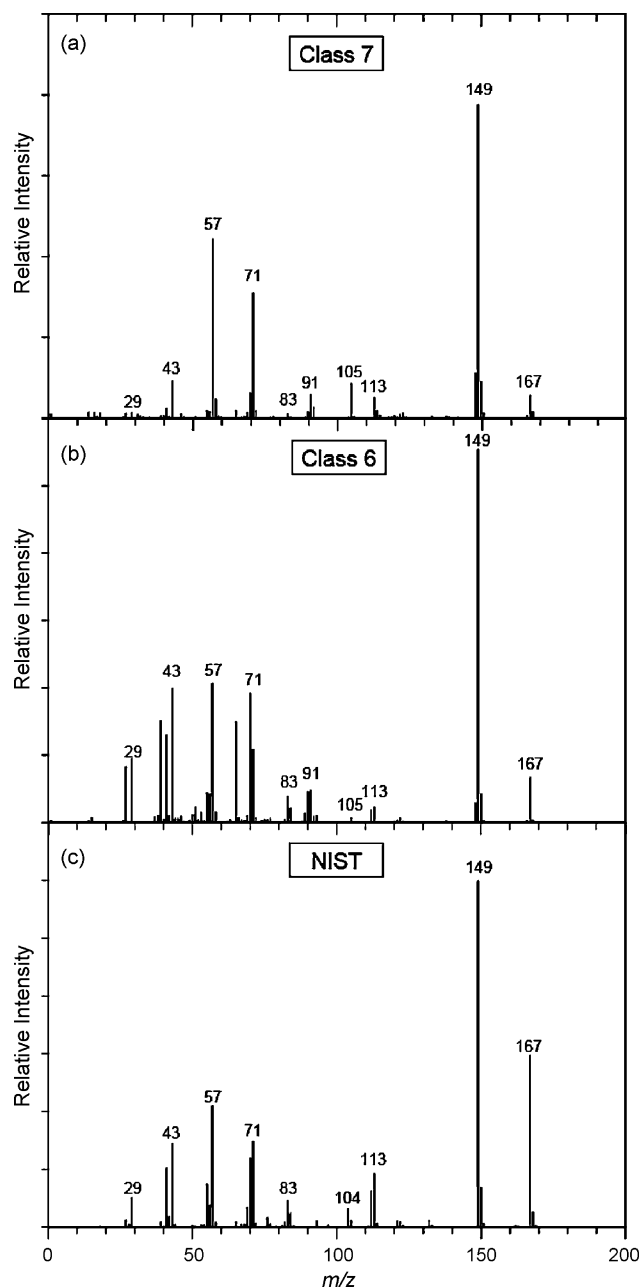


**Fig. 2.** (a) An average mass spectrum of class 7 obtained by UV laser ablation at low fluence; (b) an average mass spectrum of class 6 obtained in the IR/UV mode; and (c) a mass spectrum of gas phase DOP generated by 70 eV electron impact ionization from the NIST Standard Reference Database.

classification of individual particle mass spectra generated in both modes at this UV laser fluence. The horizontal axis represents the 12 particle classes and the vertical axis shows the time delay between the IR and UV lasers in microseconds. The colors represent the fraction of mass spectra that are classified into each of the classes as defined by the scale on the right.

An examination of the first frame, that shows the classification results for ablation generated mass spectra, reveals a wide range of fragmentation patterns. As a result, at this laser fluence 7 out of the 12 clusters have significant particle population. **Fig. 5** displays the average mass spectra of classes 1, 8 and 10 that are significantly populated when mass spectra are generated by laser ablation at this laser fluence. Class 1 contains 15% of the mass spectra and shows almost no intensity in  $m/z = 149$ , while classes 8 and 10, with 30% and 22% of the spectra, respectively, exhibit the charac-

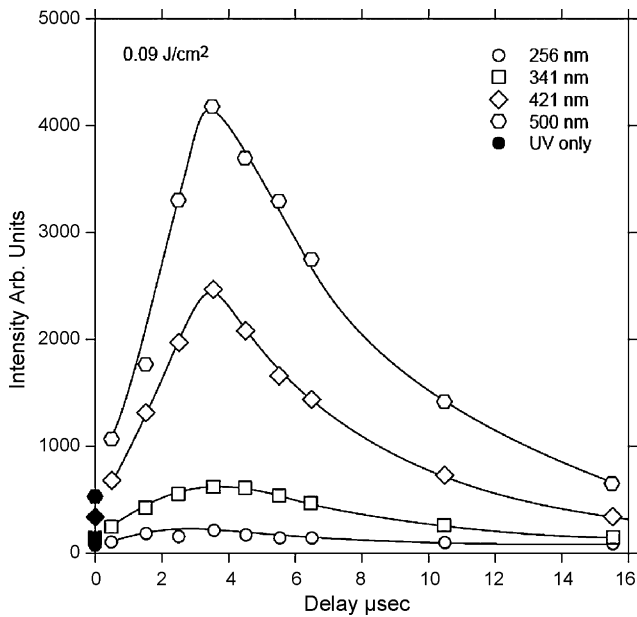


**Fig. 3.** The average integrated mass spectral intensities as a function of the time delay between the IR and UV lasers for the 4 particle sizes used in this study and laser fluence of 0.09 J/cm<sup>2</sup>. The intensities of the ablation generated mass spectra are indicated with filled symbols.

teristic phthalate peak at  $m/z = 149$ . The comparison between the ablation generated mass spectra shown in Figs. 2 and 5 illustrate that higher UV laser fluences result in an increase in the degree of fragmentation and mass spectral variability.

Returning to Fig. 4 we note that at the shortest delay times of 0.5 µs the differences between the two modes of generating mass spectra are not significant. The figure shows that at this delay a range of mass spectral fragmentation patterns are produced, resulting in significant particle population in a large number of classes. However, as the time delay between the two lasers increases and DOP evaporates the classification pattern gradually changes, such that when the delay is increased to 5.5 µs 95% of the mass spectra are in class 4. Fig. 5 shows the average mass spectrum of this class,

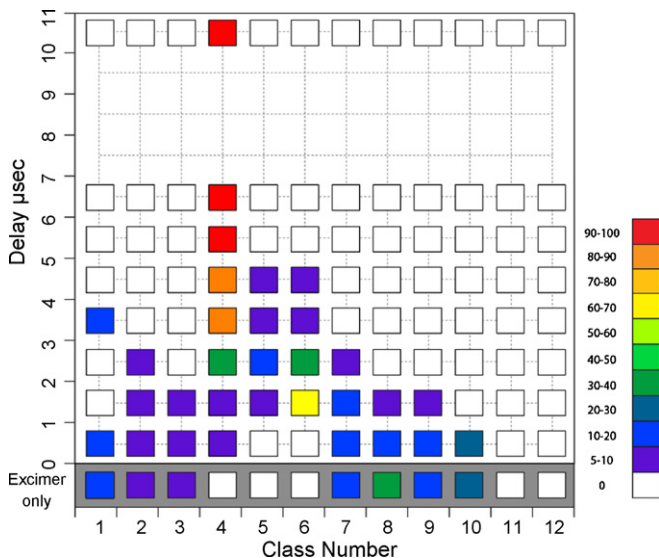


**Fig. 4.** The classification results of the mass spectra generated by ablation at laser fluence of 0.31 J/cm<sup>2</sup> are indicated in the gray frame. The rest of the figure shows the changes in the population of 12 classes as a function of the time delay between the IR and UV lasers.

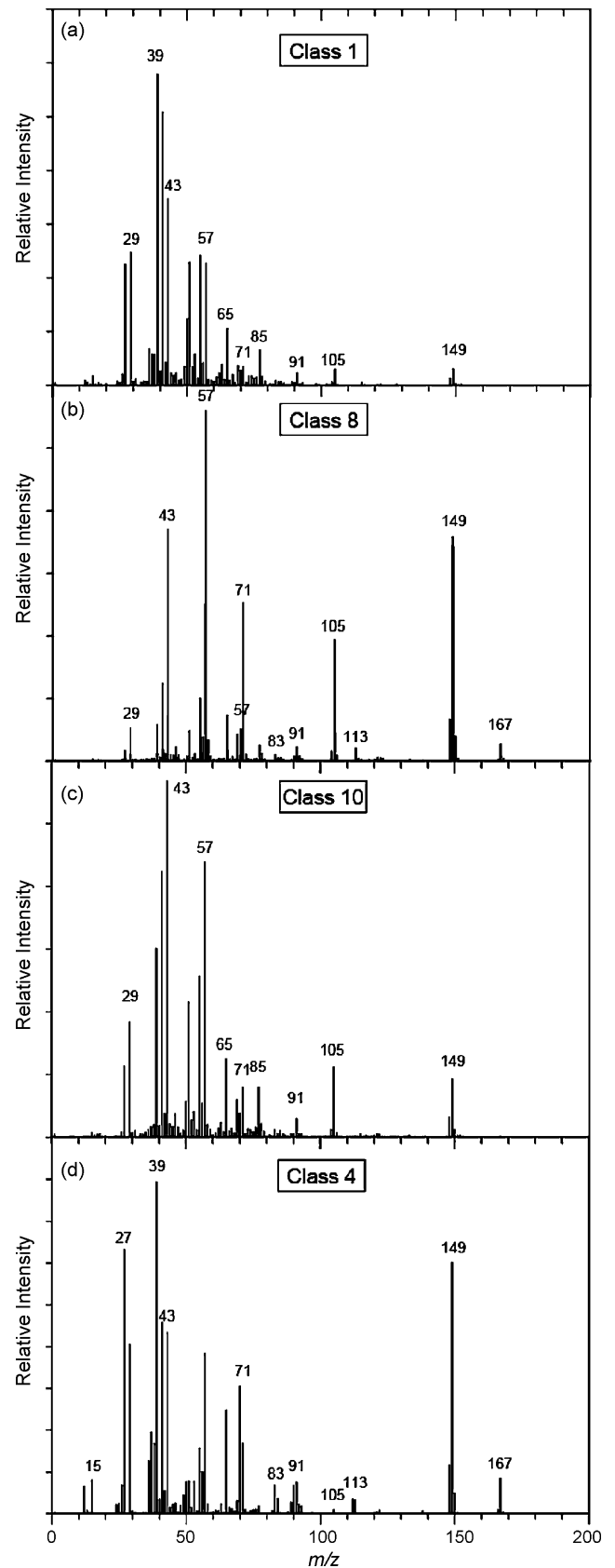


**Fig. 5.** Average mass spectra of classes 1, 8, 10, and 4.

which clearly contains the mass spectral peaks that are needed for a sound identification of phthalates. Comparison of the mass spectrum of class 4 to that of class 6 shown in Fig. 2 reveals only a slight increase in fragmentation as a result of tripling the UV laser fluence.

On the basis of the data presented in Fig. 4 we chose to focus on data that are generated at a delay of 5.5  $\mu$ s, and conclude that this delay is sufficient to shift from laser ablation to UV ionization in the gas phase only, at which point particle-to-particle mass spectral variability is nearly eliminated. Further increases in delay produce lower mass spectral intensity due to further expansion of the evaporating plume, but no improvement in mass spectral quality.

### 3.3. UV laser fluence of 0.65 J/cm<sup>2</sup> and 0.93 J/cm<sup>2</sup>

This section presents the results of measurements conducted with UV laser fluence of 0.65 J/cm<sup>2</sup> and 0.93 J/cm<sup>2</sup>. The former laser fluence is sufficient to generate mass spectra from particles composed of ammonium sulfate, but with very low probability, while the latter laser fluence represents typical UV laser power used with

SPLAT II in the field. Fig. 6 shows the results of the classification of the mass spectra generated at these UV laser fluences, by laser ablation (open bars) and in the IR/UV mode (filled bars). Focusing first on the ablation generated mass spectra, we note that at both laser fluences a significant fraction of the mass spectra populate classes 3, 11 and 12, the average mass spectra of which are shown in Fig. 7. The figure shows that all of these mass spectra exhibit extensive fragmentation and have no intensity at higher  $m/z$  ratios, including those at  $m/z = 149$  and 167. Moreover, the mass spectra of classes 11 and 12, containing 84% of the ablation generated mass spectra at 0.93 J/cm<sup>2</sup>, are dominated by a carbon clusters progression, C<sub>1</sub><sup>+</sup>, C<sub>2</sub><sup>+</sup> and C<sub>3</sub><sup>+</sup>, and are nearly indistinguishable from the mass spectra of soot particles.

In contrast with the changes observed in the ablation generated mass spectra with increased laser fluence, nearly 100% of the mass spectra generated in the IR/UV mode at these laser fluences are classified in class 4. In general, we find the fragmentation patterns

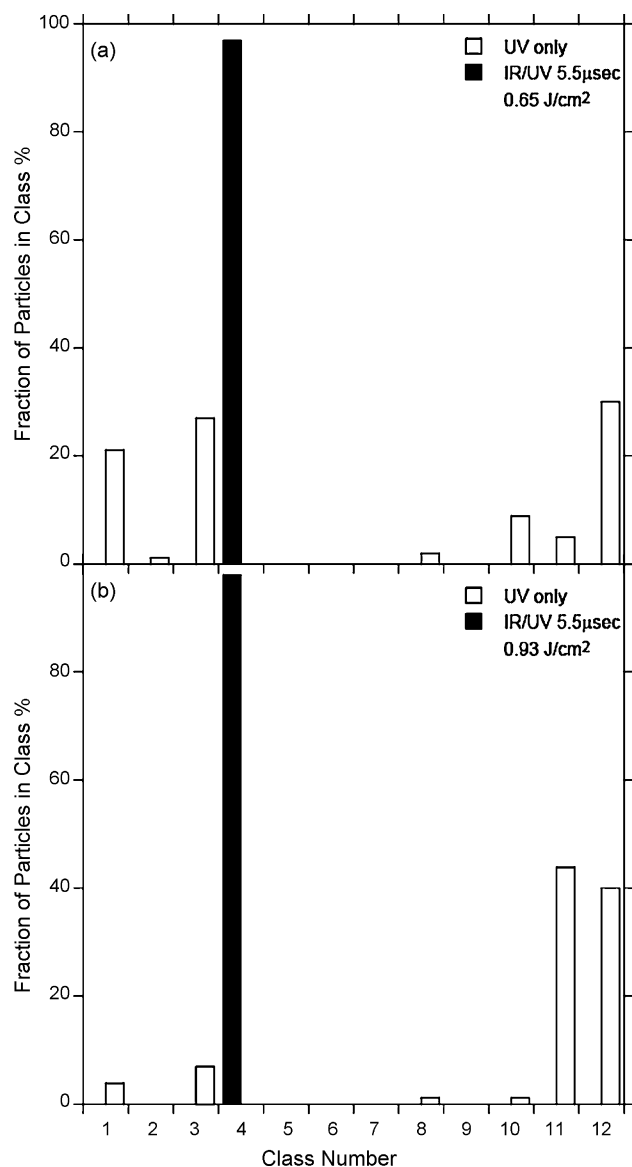


Fig. 6. The classification results of mass spectra generated by ablation and in the IR/UV mode for laser fluence of (a) 0.65 J/cm<sup>2</sup> and (b) 0.93 J/cm<sup>2</sup>.

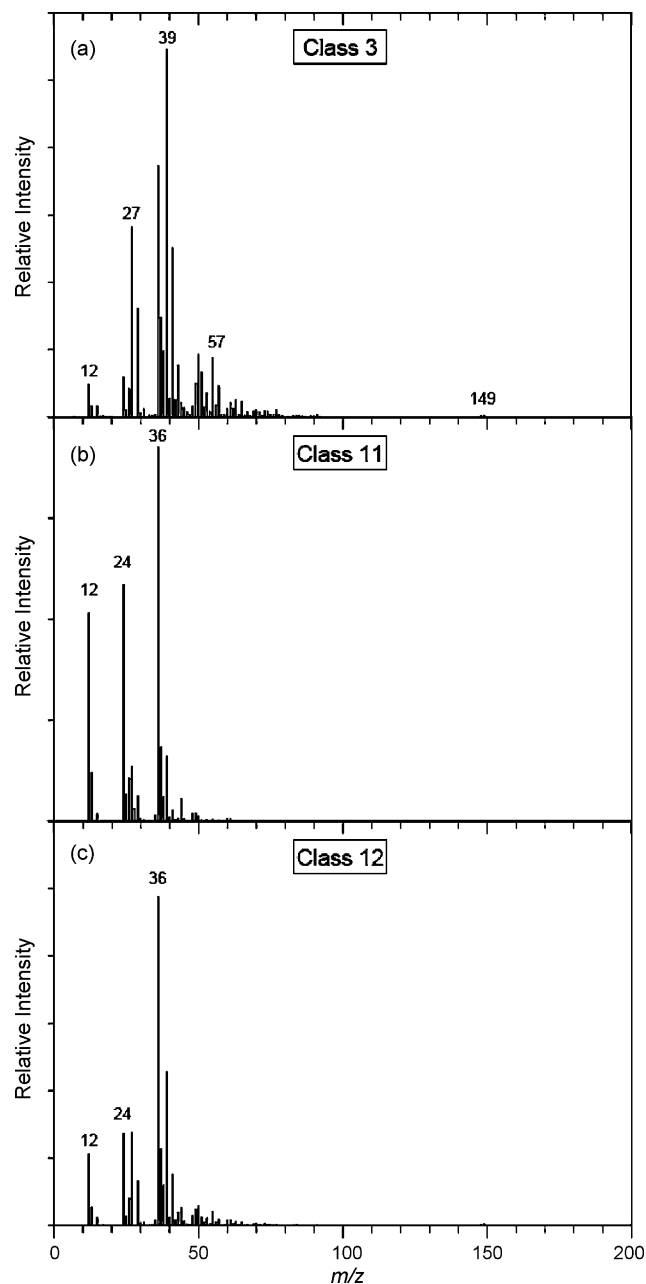


Fig. 7. Average mass spectra of classes 3, 11 and 12.

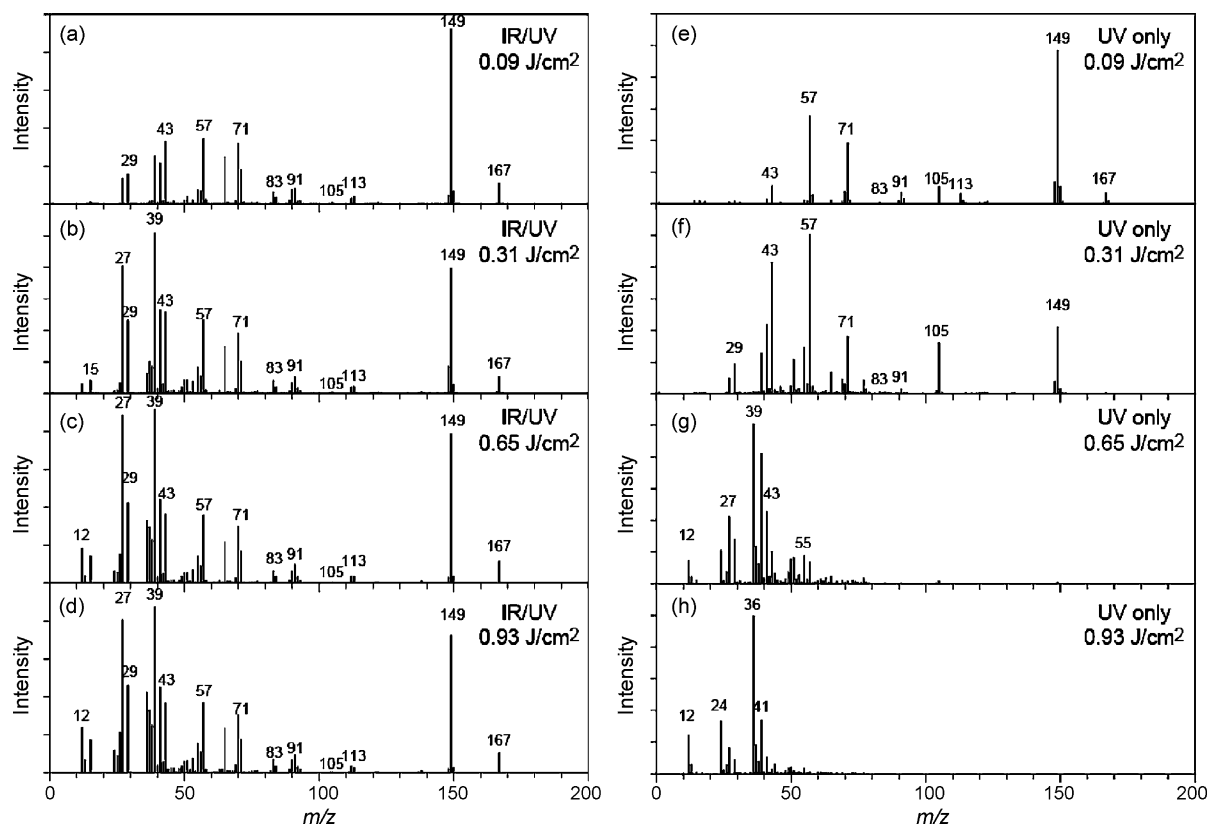


Fig. 8. Average mass spectra of 334 nm DOP particles generated by laser ablation (a–d) and in the IR/UV mode (e–h) as a function of the UV laser fluence.

of the ablation generated mass spectra to be much more dependent on the UV laser fluence than those that are generated in the IR/UV mode. Fig. 8 provides a comparison between the behaviors of the average mass spectra of 341 nm DOP particles as a function of the UV laser fluence for the two ion generation modes. As the laser fluence increases the ablation generated mass spectra, shown in Fig. 8(e)–(h) exhibit less intensity in the higher  $m/z$  and at the highest laser fluence they are dominated by the carbon clusters progression. The same order of magnitude increase in the UV laser fluence has only a slight effect on the IR/UV mass spectra and allows for easy identification of phthalates for nearly 100% of the individual particle mass spectra.

Moreover, significantly reduced fluctuations in the intensity pattern of mass spectra generated in the IR/UV mode opens the possibility to make use of the mass spectral intensities to obtain quantitative information on particle composition. Indeed, Woods et al. [35] demonstrated that the peak intensities of IR/VUV generated mass spectra of internally mixed particles composed of ternary mixtures of aromatic compounds can be used to quantify the relative amounts of these compounds. In the present study we find strong linear relationships ( $R^2 > 0.93$ ) between the average integrated intensity of mass spectra generated in the IR/UV mode and particle mass, for all four UV laser fluences. Furthermore, these linear relationships indicate that the CO<sub>2</sub> laser power that was used in this study is sufficient to entirely evaporate even DOP particles with diameters of 500 nm, despite the fact that DOP does not have a strong absorption band at the CO<sub>2</sub> laser wavelength.

#### 4. Conclusions

We presented a study of the properties and behavior of individual particle mass spectra of fine particles composed of organics. We compared the mass spectra generated by laser ablation with a UV

laser pulse at 193 nm to those generated in a two-step process, in which an IR pulse from a CO<sub>2</sub> laser is used to evaporate the particle and a time delayed UV laser pulse is used to ionize the evaporating plume. We find that the quality and information content of the ablation generated mass spectra are very sensitive to the UV laser fluence. At laser fluence that is too low to be useful for the characterization of the large fraction of atmospheric aerosol constituents the DOP mass spectra are of high quality. With the increase in the UV laser fluence the ablation generated mass spectra exhibit a high degree of fragmentation that renders these mass spectra virtually impossible to properly interpret.

In contrast, we find that the mass spectra that are generated in the IR/UV mode, with the sufficient time delay between the IR and UV to allow evaporation, are of very high quality and exhibit almost no dependence on the UV laser fluence.

Furthermore, the mass spectra generated in the IR/UV mode have approximately an order of magnitude higher integrated mass spectral intensity than those generated by laser ablation and exhibit linear relationships between the integrated mass spectral intensities and particle mass.

The classification of the data that are generated by these two methods using SpectraMiner, our data classification, analysis and visualization program, shows that the mass spectra generated by ablation tend to be classified into a large number of classes, while nearly 100% of the IR/UV mass spectra are classified in a single class that can be used to identify the particle composition.

#### Acknowledgments

This work was supported by the U.S. Department of Energy Office of Basic Energy Sciences, Chemical Sciences Division, and Energy Efficiency and Renewable Energy. This research was performed in the Environmental Molecular Sciences Laboratory, a national

scientific user facility sponsored by the Department of Energy's Office of Biological and Environmental Research at Pacific Northwest National Laboratory (PNNL). PNNL is operated by the U.S. Department of Energy by Battelle Memorial Institute under contract no. DE-AC06-76RLO 1830.

## References

- [1] K.P. Hinz, B. Spengler, *Journal of Mass Spectrometry* 42 (7) (2007) 843.
- [2] D.M. Murphy, *Mass Spectrometry Reviews* 26 (2) (2007) 150.
- [3] D.G. Nash, T. Baer, M.V. Johnston, *International Journal of Mass Spectrometry* 258 (1–3) (2006) 2.
- [4] C.A. Noble, K.A. Prather, *Mass Spectrometry Reviews* 19 (4) (2000) 248.
- [5] R.C. Sullivan, K.A. Prather, *Analytical Chemistry* 77 (12) (2005) 3861.
- [6] P.H. McMurry, *Atmospheric Environment* 34 (12–14) (2000) 1959.
- [7] D.T. Suess, K.A. Prather, *Chemical Reviews* 99 (10) (1999) 3007.
- [8] M.V. Johnston, *Journal of Mass Spectrometry* 35 (5) (2000) 585.
- [9] M. Kanakidou, J.H. Seinfeld, S.N. Pandis, I. Barnes, F.J. Dentener, M.C. Facchini, R. Van Dingenen, B. Ervens, A. Nenes, C.J. Nielsen, E. Swietlicki, J.P. Putaud, Y. Balkanski, S. Fuzzi, J. Horth, G.K. Moortgat, R. Winterhalter, C.E.L. Myhre, K. Tsigaridis, E. Vignati, E.G. Stephanou, J. Wilson, *Atmospheric Chemistry and Physics* 5 (2005) 1053.
- [10] Q. Zhang, J.L. Jimenez, M.R. Canagaratna, J.D. Allan, H. Coe, I. Ulbrich, M.R. Alfarra, A. Takami, A.M. Middlebrook, Y.L. Sun, K. Dzepina, E. Dunlea, K. Docherty, P.F. DeCarlo, D. Salcedo, T. Onasch, J.T. Jayne, T. Miyoshi, A. Shimono, S. Hatakeyama, N. Takegawa, Y. Kondo, J. Schneider, F. Drewnick, S. Borrmann, S. Weimer, K. Demerjian, P. Williams, K. Bower, R. Bahreini, L. Cottrell, R.J. Griffin, J. Rautiainen, J.Y. Sun, Y.M. Zhang, D.R. Worsnop, *Geophysical Research Letters* 34 (13) (2007) 13801.
- [11] A. Zelenyuk, J. Yang, D. Imre, E. Choi, *Aerosol Science and Technology* 43 (2009) 411.
- [12] E. Gard, J.E. Mayer, B.D. Morrical, T. Dienes, D.P. Fergenson, K.A. Prather, *Analytical Chemistry* 69 (20) (1997) 4083.
- [13] K.P. Hinz, R. Kaufmann, B. Spengler, *Aerosol Science and Technology* 24 (4) (1996) 233.
- [14] D.J. Phares, K.P. Rhoads, A.S. Wexler, *Aerosol Science and Technology* 36 (5) (2002) 583.
- [15] Y.X. Su, M.F. Sipin, H. Furutani, K.A. Prather, *Analytical Chemistry* 76 (3) (2004) 712.
- [16] D.S. Thomson, M.E. Schein, D.M. Murphy, *Aerosol Science and Technology* 33 (1–2) (2000) 153.
- [17] N. Erdmann, A. Dell'Acqua, P. Cavalli, C. Gruning, N. Omenetto, J.P. Putaud, F. Raes, R. Van Dingenen, *Aerosol Science and Technology* 39 (5) (2005) 377.
- [18] K. Park, D. Lee, A. Rai, D. Mukherjee, M.R. Zachariah, *Journal of Physical Chemistry B* 109 (15) (2005) 7290.
- [19] D.B. Kane, B. Oktem, M.V. Johnston, *Aerosol Science and Technology* 34 (6) (2001) 520.
- [20] A. Zelenyuk, J. Yang, C. Song, R.A. Zaveri, D. Imre, *Journal of Physical Chemistry A* 112 (4) (2008) 669.
- [21] Y. Cai, A. Zelenyuk, D. Imre, *Aerosol Science and Technology* 40 (12) (2006) 1111.
- [22] P.T.A. Reilly, A.C. Lazar, R.A. Gieray, W.B. Whitten, J.M. Ramsey, *Aerosol Science and Technology* 33 (1–2) (2000) 135.
- [23] D.S. Gross, M.E. Galli, P.J. Silva, K.A. Prather, *Analytical Chemistry* 72 (2) (2000) 416.
- [24] Z.Z. Ge, A.S. Wexler, M.V. Johnston, *Environmental Science & Technology* 32 (20) (1998) 3218.
- [25] A. Zelenyuk, D. Imre, Y. Cai, K. Mueller, Y.P. Han, P. Imrich, *International Journal of Mass Spectrometry* 258 (1–3) (2006) 58.
- [26] A. Zelenyuk, D. Imre, E.J. Nam, Y. Han, K. Mueller, *International Journal of Mass Spectrometry* 275 (1–3) (2008) 1.
- [27] D.B. Kane, M.V. Johnston, *Environmental Science & Technology* 34 (23) (2000) 4887.
- [28] R.J. Wenzel, K.A. Prather, *Rapid Communications in Mass Spectrometry* 18 (13) (2004) 1525.
- [29] D.S. Thomson, A.M. Middlebrook, D.M. Murphy, *Aerosol Science and Technology* 26 (6) (1997) 544.
- [30] T. Baer, J. Cabalo, A. Zelenyuk, R.E. Miller, *Abstracts of Papers of the American Chemical Society* 217 (1999) U145.
- [31] J. Cabalo, A. Zelenyuk, T. Baer, R.E. Miller, *Aerosol Science and Technology* 33 (1–2) (2000) 3.
- [32] B.D. Morrical, D.P. Fergenson, K.A. Prather, *Journal of the American Society for Mass Spectrometry* 9 (10) (1998) 1068.
- [33] A. Zelenyuk, D. Imre, *Aerosol Science and Technology* 39 (6) (2005) 554.
- [34] D.C. Sykes, E. Woods, G.D. Smith, T. Baer, R.E. Miller, *Analytical Chemistry* 74 (9) (2002) 2048.
- [35] E. Woods, G.D. Smith, Y. Dessiaterik, T. Baer, R.E. Miller, *Analytical Chemistry* 73 (10) (2001) 2317.
- [36] A. Lazar, P.T.A. Reilly, W.B. Whitten, J.M. Ramsey, *Environmental Science & Technology* 33 (22) (1999) 3993.
- [37] A. Zelenyuk, J. Cabalo, T. Baer, R.E. Miller, *Analytical Chemistry* 71 (9) (1999) 1802.
- [38] D.G. Nash, X.F. Liu, E.R. Mysak, T. Baer, *International Journal of Mass Spectrometry* 241 (2–3) (2005) 89.
- [39] E. Woods, G.D. Smith, R.E. Miller, T. Baer, *Analytical Chemistry* 74 (7) (2002) 1642.
- [40] A. Zelenyuk, D. Imre, J.H. Han, S. Oatis, *Analytical Chemistry* 80 (5) (2008) 1401.